Journal of Hydrology, 110 (1989) 51–62
Elsevier Science Publishers B.V., Amsterdam — Printed in The Netherlands

[4]

A PHYSICAL MODEL TO COMPLEMENT RAINFALL NORMALS OVER COMPLEX TERRAIN

P. ALPERT and H. SHAFIR

Department of Geophysics and Planetary Sciences, Raymond and Beverly Sackler Faculty of Exact Sciences, Tel Aviv University, Ramat Aviv 69978 (Israel)

(Received August 15, 1988; accepted after revision January 24, 1989)

ABSTRACT

Alpert, P. and Shafir, H., 1989. A physical model to complement rainfall normals over complex terrain. J. Hydrol., 110: 51–62.

A physical model for high-resolution (Δx = 1–2 km) rainfall over complex terrain that was recently verified against radar-derived observations is shown to be capable of complementing rainfall normals in Israel. Two examples illustrate that even high resolution rain-gauge networks may miss important small-scale rainfall features over highly complex terrain, which are effectively detected by a simplified linear and adiabatic model.

INTRODUCTION

The accurate prediction/diagnosis of rainfall over complex topography is one of the most difficult problems in mountain meteorology and is of special importance for hydrological applications. The characteristics of orographic rain and their favorable conditions in southern England were reviewed by Browning (1980). The feeder–seeder mechanism suggested by Bergeron (1965) was accepted as a reasonable explanation for mesoscale (typical horizontal grid interval Δ of about 10–25 km) orographic rain. Theoretical studies by Collier (1975), Storebo (1976), Bader and Roach (1977), Bell (1978), Corradini (1985), Richard et al. (1987) and others, supported this idea. However, these models as well as others over complex topography have not studied the meso-γ (classification according to Orlanski, 1975; $\Delta \sim$ 1 km) distribution of precipitation in two horizontal directions as compared with similar resolution in the observations. The reason for the latter is two-fold. First, there are large difficulties in applying a refined three-dimensional meso-γ model. Secondly, high resolution rainfall data over complex terrain are in general not available.

Alpert (1986) has shown that an adiabatic linear model with a crude parametrization of the microphysics could be used for satisfactorily indexing the distribution of orographic precipitation over two-dimensional cross sections of high mountains. Following the studies by Hill et al. (1981) and Collier and Knowles (1986), which demonstrated that high resolution orographic rainfall could be estimated from radar data, Alpert and Shafir (1989) have compared their predictions with radar-derived precipitation in Israel. The model was

0022-1694/89/$03.50

basically an extension of Alpert's (1986) model to a horizontal two-dimensional plane that follows the terrain. Alpert and Shafir applied their model to some case studies as well as annual averages over highly rugged terrain.

The purpose of the present study is to illustrate how the Alpert–Shafir model could be used to complement rainfall data over complex topography. One case is for the Judean Mountains normals, i.e. annual averages, following Alpert–Shafir and the second is for the Galilee Mountains with horizontal resolutions of 2 and 1 km respectively. Following the two cases is a discussion of the advantages of the model for diagnosis/prediction of rainfall distribution over complex terrain and the suggestion to combine statistical and physical models.

FIRST CASE — THE JUDEAN MOUNTAINS

The general region and the two study domains, i.e. the rectangles in the Judean and Galilee mountains, are shown in Fig. 1. The two hilly domains are part of an approximately north–south mountain line running parallel to the southeastern Mediterranean coast at a distance of 20–40 km. The topography is illustrated by the 300 m contours (dashed lines). The study domain for the first example is a 30 × 60 km rectangle and is enlarged in Fig. 2. The grid interval was $\Delta x = \Delta y = 2$ km. Rainfall averages for the winter rain season exceed 700 mm, while upstream, along the coast, values are in the range of

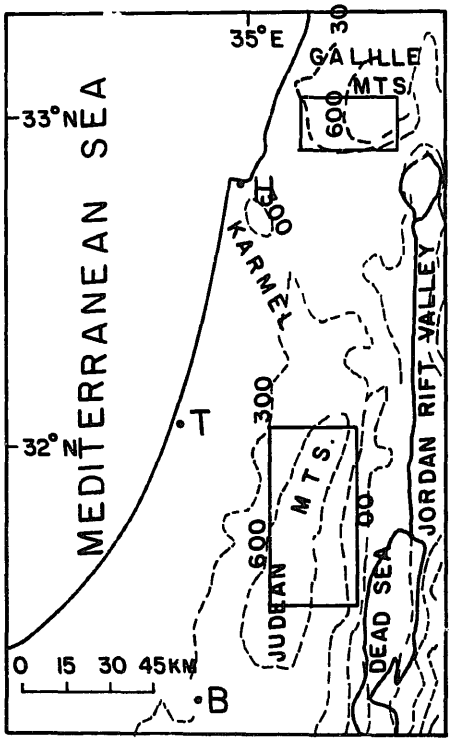

Fig. 1. General location of the study area. Topographic contours are at 300 m intervals. Rectangular areas denote the two study domains. Letters *H*, *T*, and *B* represent the towns of Haifa, Tel Aviv, and Beer-Sheva respectively.

400–500 mm (e.g. Wolfson, 1975). The rainfall enhancement over the mountains is particularly high later in the winter as the coastal contribution diminishes and the mountainous rainfall may even become double or more than the corresponding amounts on the coast (2–5 times more in a February case study discussed in Alpert and Shafir, 1989).

Areas exceeding 800 m in elevation are shaded (Fig. 2) and locations of rain gauges are denoted. The 29 crossed stations were not used for case studies (not

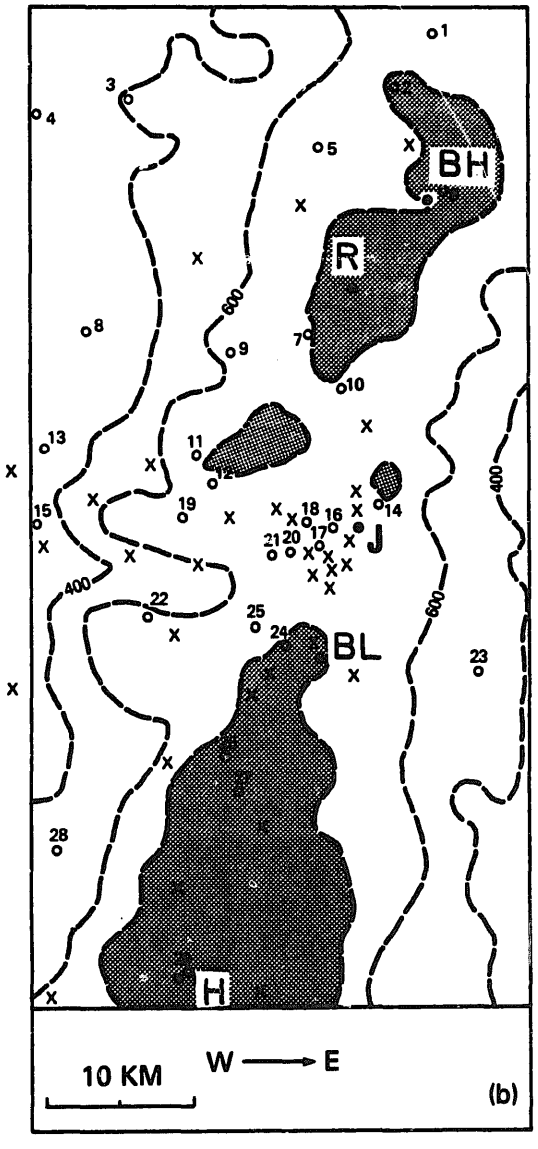

Fig. 2. Study area for the first case — the Judean Mountains. Topographic contours are at 200 m intervals. Shading represents elevations higher than 800 m. The circles and crosses denote gauges which are used in the present study. Twenty-nine stations (circled) were used in the case studies reported by Alpert and Shafir (1989). Locations *R*, *BH*, *J*, *BL* and *H* represent Ramalla, Baal-Hatsor, Jerusalem, Bethlehem and Hebron respectively.

TABLE 1

Input parameters for the model used in the two cases discussed

Experiment	Rainfall		Wind (deg/m s^{-1})	Upstream precipitation P_0 (mm)	MSL temperature T_0 (K)	Lapse-rate (°C km^{-1})	Relative humidity (RH) variation upstream (%)		RH at MSL(%) (northwest corner)
	Period	Efficiency					Horizontal (y-north)	Vertical (z-upward)	
1 Judea	47 d*	0.1	270/10	550	291	6.5	+30 (also −15 in the x-direction)	0	100
2 Galilee	62 d*	0.075	225/10	570	291	6.5	0	0	100

*Based on average annual number of rainfall days in the area.

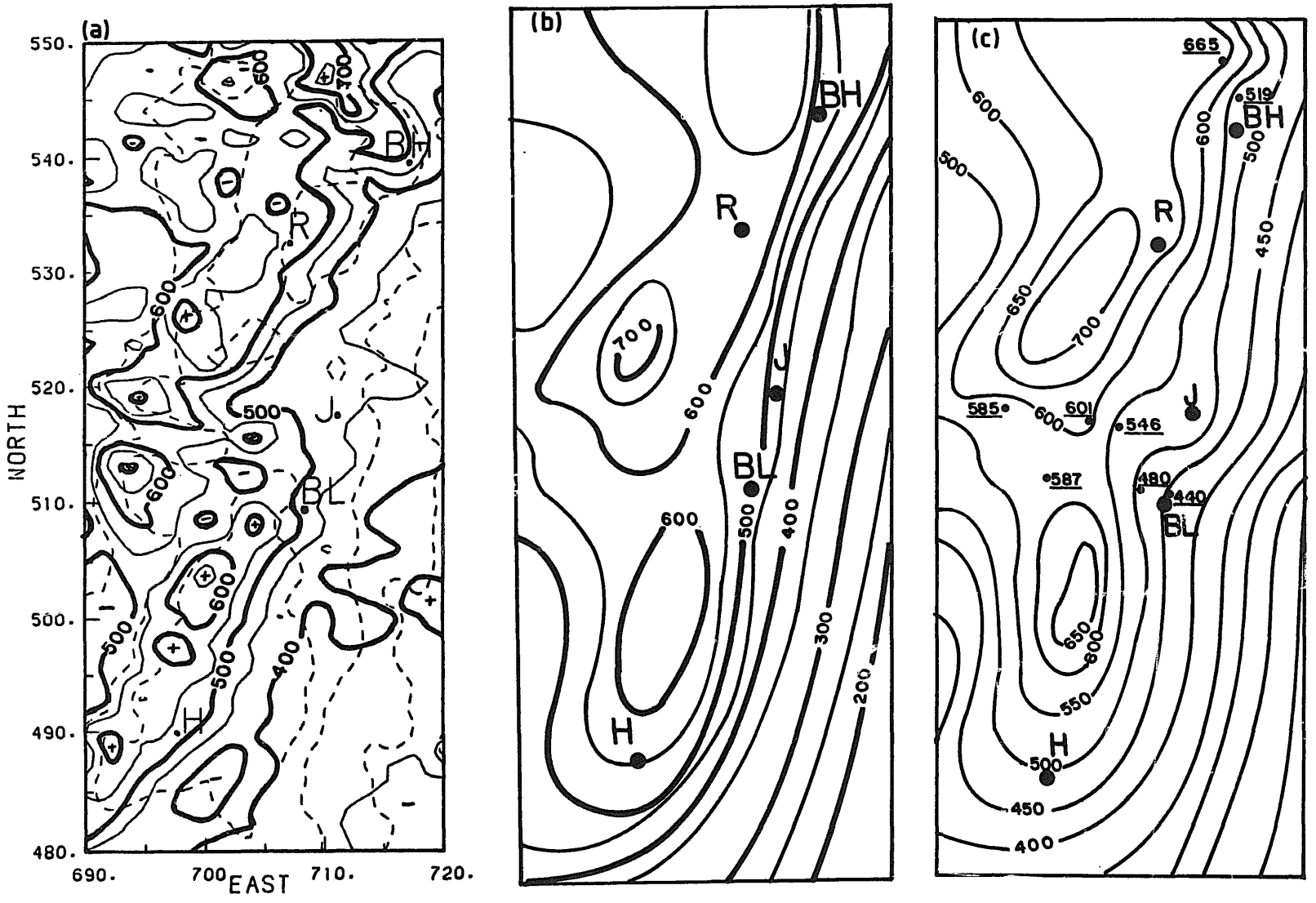

Fig. 3. (a) Contours of average annual rainfall from the model. Dashed lines are topographic contours at 200 m intervals, grid numbers are in kilometers and the contour interval is 50 mm yr^{-1}. (b) Observed contours of average annual rainfall based on data from about 58 gauges (Fig. 2) during the period 1951–1980. This was taken from an IMS map (Israel Meteorological Service, 1985). The contour interval is 50 mm yr^{-1}. (c) Same as (b) but from the IHS map (Israel Hydrological Service, 1981). The observed rainfall normals at some stations are also indicated. All three frames cover the same area shown as the southern rectangle in Fig. 1.

presented here). Locations R, BH, J, BL and H represent Ramalla, Baal-Hatsor, Jerusalem, Bethlehem and Hebron.

The model equations, input parameters and other numerical and physical aspects are found in detail in Alpert (1986) and Alpert and Shafir (1989). Some of the relevant parameters are shown in Table 1. The model-simulated and observed average annual rainfall rates are shown in Figs. 3a and b–c respectively. Figures 3b and c are based upon 58 gauges for 1951–1980 from the IMS/IHS (Israel Meteorological/Hydrological Service) respectively. Both analyses are subjective but in the IHS map more emphasis was put on the smaller scale features. This will be later discussed.

The model results, Fig. 3a, indicate the basic features of the observed distribution, such as the location of the 700 mm yr^{-1} maximum on a rainfall ridge from the north toward the southwest. Notice also the 600 mm yr^{-1} contour southwest of BL which extends in the southwesterly direction and the minimum of 500 mm yr^{-1} to its west. Of major concern here, however, are the many smaller-scale features which appear in the model simulation but do not exist in the observations. Some examples follow.

(1) The most prominent difference is probably due to the 700 mm maximum at coordinates (693,513) of Fig. 3a, far to the west of BL. Not only does this maximum not appear in Figs. 3b and c — derived from observations — but it seems to be in the region of a minimum. A closer look at the site (Fig. 2) reveals that this area does not contain any reporting stations. Presumably this fact explains the apparent contradiction between the model and the observations. It also exemplifies how the model could complement the observations. In this case, it strongly suggests substituting the relative minimum west of BL (Figs. 3b, c) by the maximum of 700 mm yr^{-1} predicted by the model.

(2) At the northeastern domain edge near BH, a trough of minimum rainfall extends from slightly south of BH towards the northwest. Similarly, a ridge of maximum rainfall with a maximum of 750 mm yr^{-1} extends southeast, directly towards BH. The IMS map (Fig. 3b) does not contain the ridge and trough at all, but the IHS map (Fig. 3c) does indicate this feature, which is much weaker than the model predicted. This is not surprising when one notices that only 2–3 gauges exist in this complex topographical region. In particular, one station reports 665 mm yr^{-1} compared to only 519 mm yr^{-1} for the more southerly station located right in the rainfall trough (Fig. 3c). Subjective analyses of such apparently contradicting reports could result in one of two courses: Either disregard the large difference as was done in Fig. 3b, or strongly bend the isohyets in order to take into account both reports, i.e. Fig. 3c. Obviously, in this case the model supports the second approach.

(3) From BL a rainfall trough extends northwest along with a neighbouring ridge to its north, which extends from point (694,519) towards the east-southeast and reaches the area slightly south of J (Fig. 3a). The trough and ridge do appear in Fig. 3c, where small differences were considered, but not in Fig. 3b. However, a second rainfall trough in the model, which extends from north of J towards the west (Fig. 3a), does not exist in either of the observations

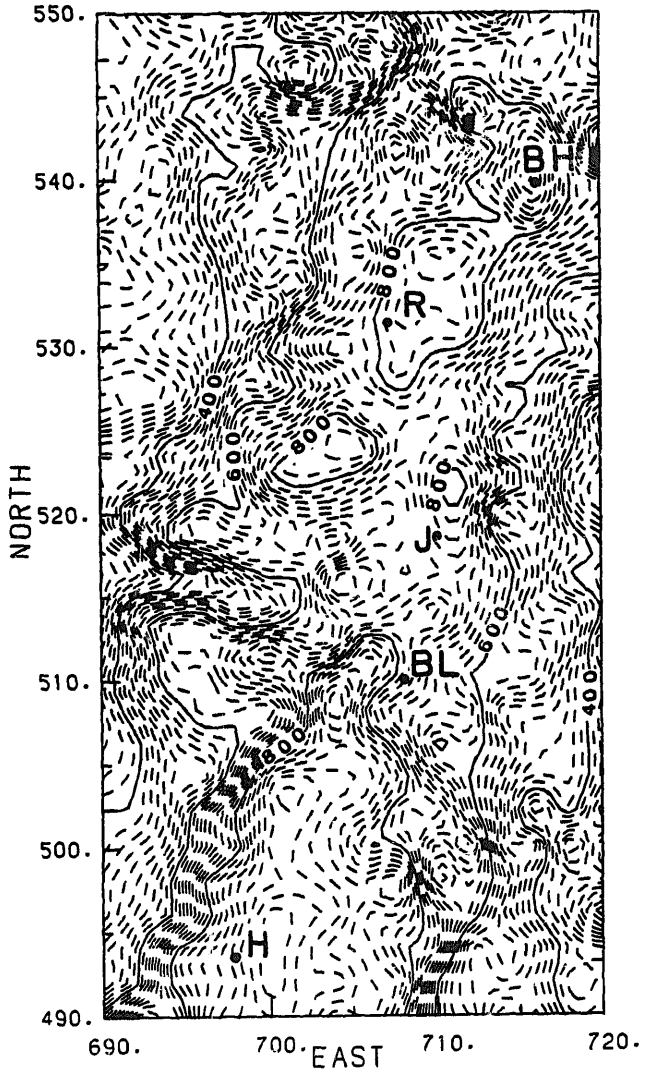

Fig. 4. Study domain-the Judean Mountains. Dashed topographic contours are at 20 m intervals and the solid lines are at 200 m intervals, as in Fig. 2.

analyses. Again, inspection of Fig. 2 reveals the lack of observations in that region (north of stations 16 and 18 in Fig. 2).

The three examples illustrate how the model's predicted distribution presents much more detail on a smaller scale. Obviously, the major source of this detail is the high-resolution complex topographical features incorporated in the model. Figure 4 shows the high-resolution topographical features (contour interval of 20 m) which the model incorporates. For instance, the topographical ridge extending west of BL towards point (693,513) could certainly explain the model maximum there while the absence of this maximum in the observations is clearly the result of a lack of rain-gauges over this mountain ridge (compare with Fig. 2).

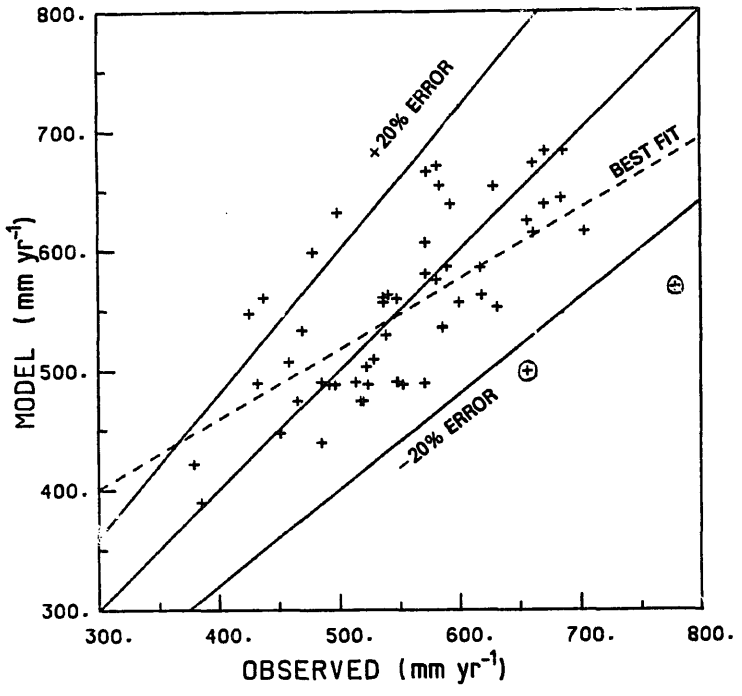

Fig. 5. Correlation between modeled and observed average annual rainfall for the Judean Mountains case. Best fit curve is given by $y = 0.59\,x \pm 225$ with a correlation of 0.67. Lines of ± 20% error are indicated. Without the two circled points, the correlation factor increases to 0.74.

The correlation between the modeled and observed average annual rainfall for all raingauges is presented in Fig. 5. From 58 stations, only six have errors which are larger than 20% and the coefficient of correlation is 0.67, with a significance level of 99% (it increases to 0.74 when the two circled stations are omitted — the values for these stations were suspected to be wrong). It should be stressed that the model output was obtained without using any of the available rainfall data. Later, the option of blending physical and statistical results will be discussed.

SECOND CASE — THE GALILEE MOUNTAINS

The location of this simulation is depicted generally in Fig. 1 and detailed in Fig. 6. Topographic contours with a 200 m interval are shown and areas exceeding 800 m in elevation are shaded. Crosses indicate available rain-gauge stations. Locations JN, MR, SS, ZF and KN represent Bet-Jan, Har-Meron, Sasa, Zefat and Har-Kenaan, respectively. Some of the input parameters for the model run are shown in Table 1. A 33 × 18 km rectangle was adopted with a horizontal grid interval of 1 km, as indicated in Fig. 6. The model-simulated and observed average annual rainfall rates are shown in Figs. 7a and b–d, respectively. Figures 7b and c are IMS maps for 1931–1960 and 1951–1980 respectively, while Fig. 7d is the IHS map for 1951–1980. The differences between Figs. 7b and

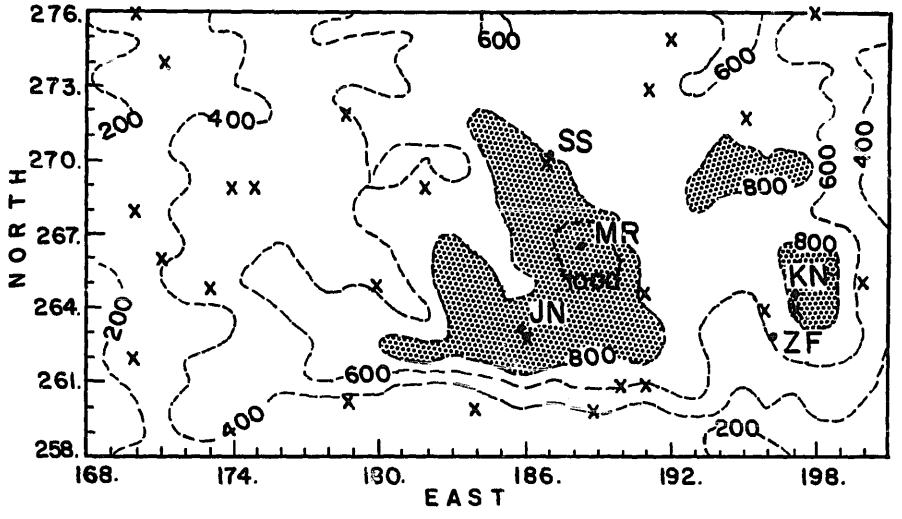

Fig. 6. Study domain for the second case — the Galilee Mountains. Topographic contours are at 200 m intervals. Shaded regions are higher than 800 m. The crosses denote rain-gauge locations. Letters JN, MR, SS, ZF and KN represent Beth-Jan, Har-Meron, Sasa, Zefat and Har-Kenaan respectively.

c are probably strongly related to the seeding project (e.g., Gagin and Gabriel, 1987), and to the enhanced urbanization which took place during the latter period (1951–1980). These effects are discussed in a separate study by Shafir and Alpert (1989).

As expected from the first case, the model reflects the basic features of the observed distribution; e.g., the major maximum near MR along with its extensions to the east and west (Fig. 7a). Also, the sharp north–south rainfall gradient south of JN and minimum rainfall trough at the northeastern section of the domain, which extends to the west, are reasonably simulated. But, as before, the model's predicted distribution includes many smaller-scale features which sometimes are reflected in the observed maps, in particular the IHS map, but in general cannot be found in the observations, probably due to lack of high-resolution rainfall data. Some examples follow.

(1) The rainfall maximum which extends northwards from JN + MR to SS, as illustrated in the model prediction (Fig. 7a), does not exist in the observational maps, although the IHS map does show a weak ridge. Examination of the location of rain-gauges (Fig. 6) shows that data in that region are not available.

(2) Similarly, the + 900 mm maximum at (173,260) in Fig. 7a is missing in the observed maps. Again, Fig. 6 verifies the lack of rainfall data there.

(3) Between the stations of MR and ZF, the model predicts a relative minimum, below 800 mm, and a secondary maximum east of it. This minimum is missing in the observational maps (Figs. 7b–d) and this could also be at least partly explained by the lack of rain-gauges in the valley between MR and ZF.

The correlation between the modeled and observed rainfall values for all the rain-gauge data available is presented in Fig. 8. From 25 stations, only 3 have errors larger than 20% and the coefficient of correlation is 0.61, with a sig-

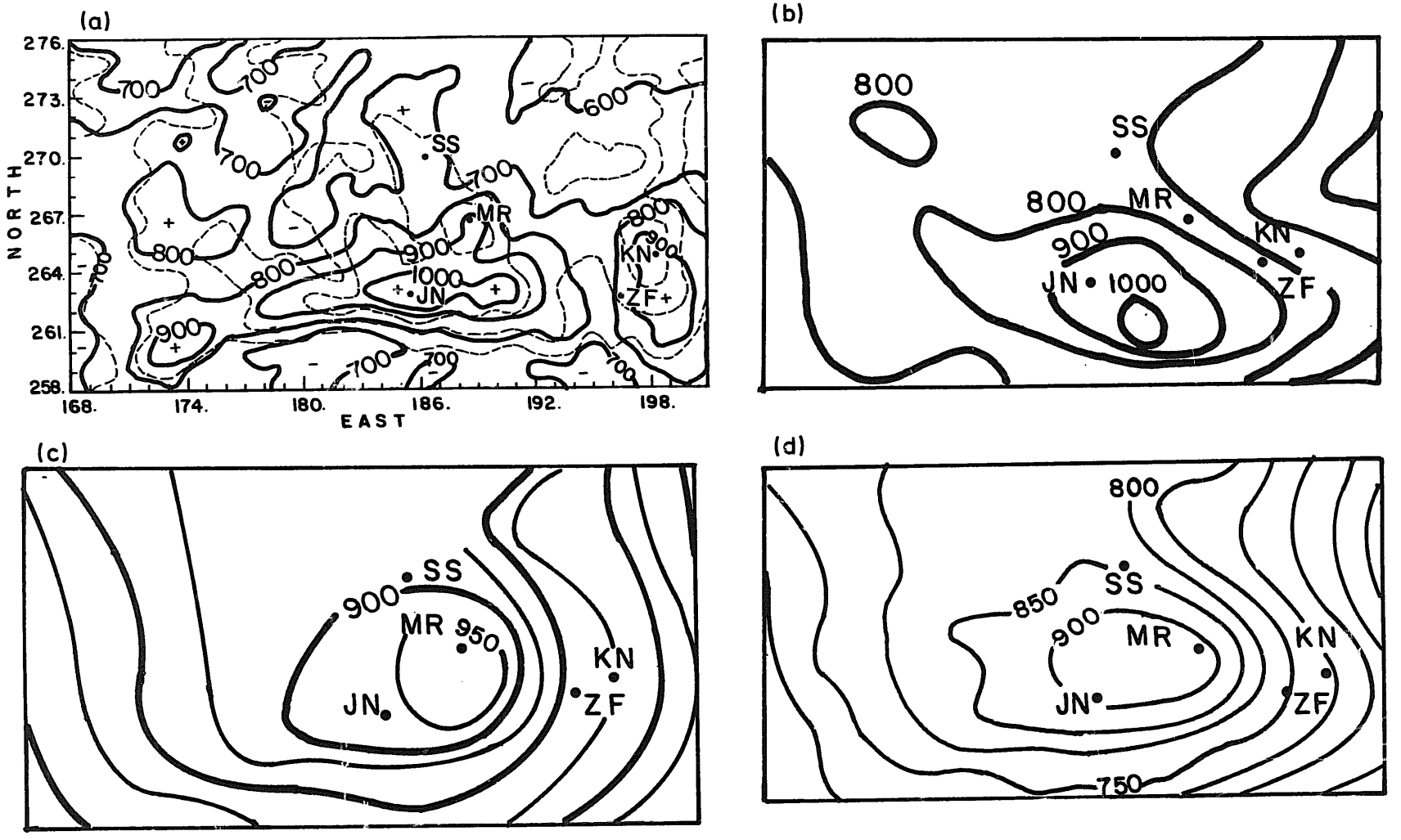

Fig. 7. Contours of average annual rainfall at intervals of 100 mm yr^{-1}, derived from: (a) The model shown on the base map in Fig. 6. (b) Israel Meteorological Service (1964), for the period 1931–1960. (c) Israel Meteorolgical Service (1985), for the period 1951–1980 (d) Israel Hydrological Service (1981), for the period 1951–1980. The contour interval in c–d is 50 mm yr^{-1}.

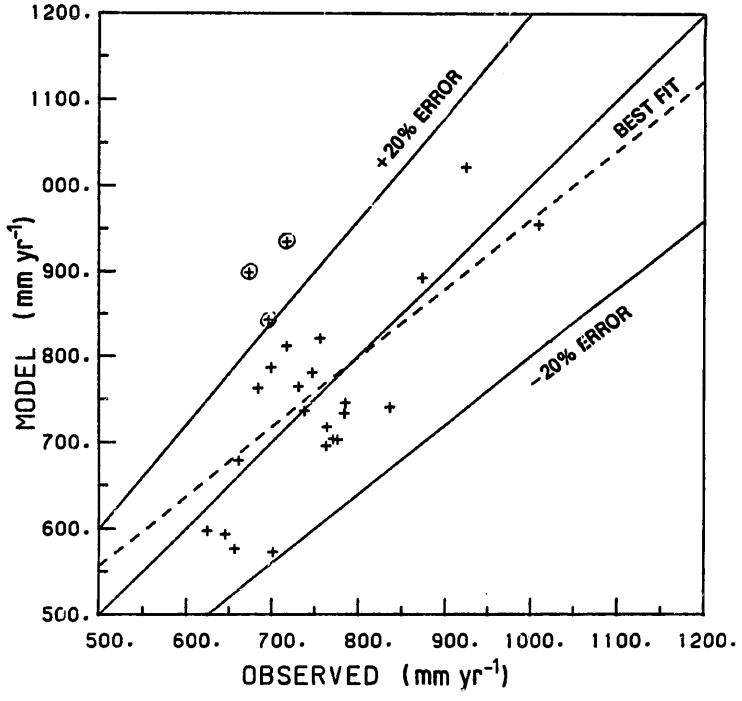

Fig. 8. Correlation between modeled and observed average annual rainfall for the Galilee Mountains case. Best fit curve is given by $Y = 0.8X + 153$ with a correlation of 0.61. Lines of ± 20% error are indicated. Without the three circled points, the correlation factor increases to 0.80 and the best fit curve becomes $Y = 0.99X - 8$.

nificance level of 99% (it increases to 0.80 when the 3 circled stations are omitted). The best fit line is given by $Y = 0.8X + 153$ (dashed line in Fig. 8) or $Y = 0.99X - 8$ when excluding the three circled stations. Y and X stand for theoretical and observed rainfall respectively.

SUMMARY AND DISCUSSION

To the best of our knowledge, the physical (Alpert–Shafir) model applied here was the first to verify rainfall patterns on the small meso-γ scale over complex terrain against radar data. The current work has illustrated, through annual averages, how the physical model detects high-resolution features of the rainfall distribution which do not exist in the observational maps. It should be noted that although the two study domains have a relatively high density of rain-gauges, important features of rainfall distribution predicted by the model were missing. The reason is suggested to be the highly complex topography which is very difficult, if not impossible, to cover effectively with a network of rain-gauges.

The current model did not make use at all of the observations available and yet has achieved relatively high correlation coefficients. Hence, we expect that the model could be effectively used in conjunction with statistical models to

complement rainfall averages in data-free regions. Also, in the planning of rain-gauge networks, the model output can serve as an initial guide for regions of high and low gradients of precipitation.

ACKNOWLEDGMENTS

We wish to thank the Israel Meteorological and Hydrological Services for supplying the data. Thanks to the BSF (Bi-National U.S.–Israel Science Foundation) for partly supporting H. Shafir through grant No. 8600230. Many thanks to Ms. Rachel Duani for typing the manuscript and Mr. A. Dvir for drafting the figures.

REFERENCES

Alpert, P., 1986. Mesoscale indexing of the distribution of orographic precipitation over high mountains. J. Clim. Appl. Meteorol. 25: 532–545.

Alpert, P. and Shafir, H., 1989. Meso-γ scale distribution of orographic precipitation: Numerical study and comparison with precipitation derived from radar measurements. J. Appl. Meteorol., vol. 28

Bader, M.J., and Roach, W.T. 1977. Orographic rainfall in warm sectors of depressions. Q. J. R. Meteorol. Soc., 103: 269–280.

Bell, R.S., 1978. The forecasting of orographically enhanced rainfall accumulations using 10-level model data. Meteorol. Mag., 107: 113–124.

Bergeron, T., 1965. On the low-level redistribution of atmospheric water caused by orography. Suppl. Proc. Int. Conf. Phys., Tokyo, pp. 96–100.

Browning, K.A., 1980. Structure, mechanism and prediction of orographically enhanced rain in Britain. In: R. Hide and P.W. White (Editors), Orographic effects in planetary flows. Global Atmos. Res. Proj. Publ. Ser. 23, pp. 85–114.

Collier, C.G., 1975. A representation of the effects of topography on surface rainfall within moving baroclinic disturbances. Q.J.R. Meteorol. Soc., 101: 407–422.

Collier, C.G. and Knowles, J.M., 1986. Accuracy of rainfall estimates by radar. Part II: Application for short-term flood forecasting. J. Hydrol., 83: 237–249.

Corradini, C., 1985. Analysis of the effects of orography on surface rainfall by a parametrized numerical model. J. Hydrol., 77: 19–30.

Gagin, A. and Gabriel, K.R., 1987. Analysis of recording rain-gauge data for the Israeli II experiment. Part I: Effects of cloud seeding on the components of daily rainfall. J. Climatol. Appl. Meteorol., 26: 913–921.

Hill, F.F., Browning K.A., and Bader, M.J., 1981. Radar and rain-gauge observations of orographic rain over south Wales. Q.J.R. Meteorol. Soc., 107: 643–670.

Orlanski, I., 1975. A rational subdivision of scales for atmospheric processes. Bull. Am. Meteorol. Soc., 56: 527–530.

Richard, E., Chaumerliac, N., Mahfouf J.F., and Nickerson, E.C., 1987. Numerical simulation of orographic enhancement of rain with a mesoscale model. J. Clim. Appl. Meteorol., 26, 661–669.

Shafir, H., and Alpert, P., 1989. On the urban orographic rainfall anomaly in Jerusalem – A numerical study. Atmos. Environ. (in prep.).

Storebo, P.R. 1976. Small scale topographic influences on precipitation. Tellus, 28: 45–49.

Wolfson, N., 1975. topographical effects on standard normals of rainfall over Israel. Weather, 30: 138–144.